Sensors and Materials, Vol. 33, No. 6 (2021) 2171–2178
MYU Tokyo

S & M 2604

Luminescence Properties of Eu:$KCaPO_4$ Ceramics That Generate New Luminescent Centers upon X-ray Irradiation

Daiki Shiratori,* Takumi Kato, Daisuke Nakauchi,
Noriaki Kawaguchi, and Takayuki Yanagida

Nara Institute of Science and Technology, 8916-5 Takayama, Ikoma, Nara 630-0192, Japan

(Received January 31, 2021; accepted May 10, 2021)

Keywords: KCaPO4, radio-photoluminescence, photoluminescence, dosimetry, ceramics

A series of $K(Eu_xCa_{1-x})PO_4$ (x = 0.001, 0.003, 0.01, and 0.03) phosphors were synthesized by the conventional solid-state reaction. To evaluate the phase purity of the as-prepared materials, X-ray diffraction (XRD) patterns were obtained. Additionally, the photoluminescence (PL) excitation/emission spectra, PL decay curves, and thermally stimulated luminescence (TSL) glow curves were studied. The PL spectrum of each specimen showed only characteristic emissions attributed to Eu^{3+}, whereas additional broad emission attributed to Eu^{2+} appeared after X-ray irradiation. This is clear evidence of radio-photoluminescence (RPL) since new luminescence centers were generated by X-ray irradiation. The RPL emission was pronounced in the 0.1% Eu-doped specimen and decreased with increasing Eu concentration.

1. Introduction

Phosphors have a very wide range of applications including lighting, displays, and sensors that use stress luminescence. Several types of phosphors are used in radiation detection applications.[1–4] Some phosphors have the function of accumulating carriers, and their emission is used in luminescence-type dosimeters. Furthermore, there are two types of such dosimeters, classified by the way in which carriers are stimulated: thermally stimulated luminescence (TSL) dosimeters use thermal stimulation[5–7] and optically stimulated luminescence (OSL) dosimeters utilize optical stimulation.[8,9] These two types of dosimeters have been widely used for personal dose monitoring. In addition, glass dosimeters using radio-photoluminescence (RPL) are practically used.[10] In the RPL phenomenon, new luminescence centers are generated via interactions with ionizing radiation.[11–13] Therefore, RPL can be easily measured by a photoluminescence (PL) technique. Practical RPL dosimeters have some advantages over conventional TSL and OSL dosimeters: RPL dosimeters show almost no fading and can be read repeatedly. Although RPL materials have some advantages over current materials, the number of materials that exhibit RPL is still limited, and there is much room for material research.

Recently, $KCaPO_4$ doped with rare earths have been attracting attention as new phosphors for radiation measurement.[14,15] In particular, it has been reported that Eu-doped $KCaPO_4$

*Corresponding author: e-mail: shiratori.daiki.sc3@ms.naist.jp
https://doi.org/10.18494/SAM.2021.3317

ISSN 0914-4935
https://myukk.org/

(Eu:$KCaPO_4$) can contain doped Eu luminescent centers in both the divalent and trivalent states depending on the preparation conditions.[16] This suggests that Eu:$KCaPO_4$ is potentially an RPL material. In this paper, we report on Eu:$KCaPO_4$ ceramics as new RPL materials.

2. Materials and Methods

2.1 Sample preparation

Ceramic specimens of $K(Eu_xCa_{1-x})PO_4$ (x = 0.001, 0.003, 0.01, and 0.03) were synthesized by the conventional solid-state reaction as follows. K_2CO_3 (4N), $CaCO_3$ (4N), $NH_4H_2PO_4$ (2N), and Eu_2O_3 (5N) powders were used as the starting materials. These powders were homogeneously mixed in the stoichiometric ratio. The mixture was calcined using an electric furnace (FTV-1700G, Full-Tech Furnace Co., Ltd.) at 650 °C for 6 h in air. Next, the product was ground and then molded into pellets by applying a uniaxial pressure of 20 MPa for 20 min using a Mini-Lab-Press (Labnect Co., Ltd.). The compressed powder pellets were then sintered in the furnace at 1100 °C for 4 h in air to obtain solid ceramic specimens.

2.2 Evaluation methods

The crystalline structure of the obtained ceramic specimens was confirmed by X-ray diffraction (XRD) measurement using a diffractometer (Miniflex 600, Rigaku). PL and RPL spectra were obtained using our lab-constructed setup. A xenon lamp (LAX-C100, Asahi Spectra) and an optical band-pass filter (RR0340, Asahi Spectra) were used to obtain a 340 nm excitation light. The PL and RPL emission spectra were obtained with an optical short-cut filter (LU0400, Asahi Spectra) and fiber-coupled lens, which guided the light to a CCD-based spectrometer (QEPro, Ocean Optics). In order to measure the RPL, X-rays with different doses were irradiated to the specimens using an X-ray generator (XRBOP&N200X4550, Spellman), and then the emission spectra were obtained using the same optics as for the PL. A spectrofluorometer (FP8600, JASCO) was used to obtain the PL and RPL excitation spectra.

The PL lifetime was obtained by decay curve measurements conducted using a Quantaurus-Tau spectrometer (C11367-04, Hamamatsu). A TL-2000 (Nanogray) TSL measuring device was used to measure TSL properties after the specimens were irradiated with X-rays.[17] The measurements were performed in the temperature range of 50–490 °C and the heating rate was 1 °C/s.

3. Results and Discussion

Calcium potassium orthophosphate is a polymorphic crystal known to exist in three forms: α-$KCaPO_4$, β-$KCaPO_4$, and $KCaPO_4$.[18,19] The XRD patterns of all the specimens and the standard Powder Diffraction Files (PDFs) of $KCaPO_4$ (No. 33-1002) and β-$KCaPO_4$ (No. 03-0618) are shown in Fig. 1. The patterns in (a) show the entire measurement range and the patterns in (b) show enlargements of the peaks around 30–33°. The peaks of $KCaPO_4$ and β-$KCaPO_4$

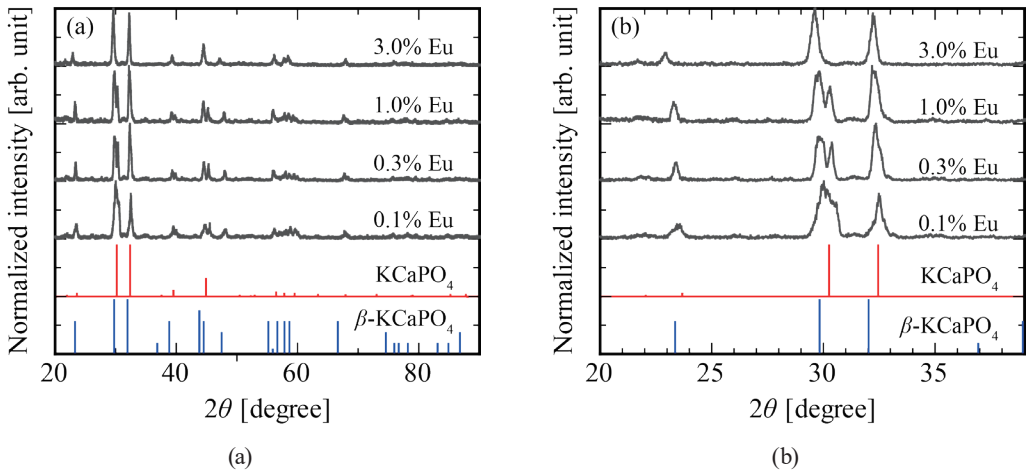

Fig. 1. (Color online) XRD patterns of each specimen (a) within the range of 20–90° and (b) at low angles.

were found to coexist in the XRD patterns of all the Eu-doped specimens. When Eu:$KCaPO_4$ is synthesized in an inert gas, no hetero-phase or peak shift occurs.[16,20] Our results suggest that β-$KCaPO_4$ appears if Eu:$KCaPO_4$ is synthesized in air. Furthermore, each diffraction peak shifted to the low-angle side with increasing Eu concentration in the specimen. It is considered that this peak shift was caused by the substitution of Eu ions at the Ca sites and the expansion of the crystal lattice by the Eu ions.

Figure 2 compares the PL spectra of all Eu-doped specimens measured before and after X-ray irradiation (10 Gy). The excitation wavelength was 340 ± 20 nm. The PL spectra of the 0.1, 0.3, and 1.0% Eu-doped specimens showed significant differences before and after X-ray irradiation. These spectral changes were more pronounced in the specimens with lower Eu concentrations and were negligible in the 3.0% Eu-doped specimen. Next, we discuss the obtained spectra. Only sharp line emissions were observed in the wavelength region of 350–500 nm. These emission features are typical for the 4*f*–4*f* transitions of Eu^{3+}. On the other hand, an additional broad emission appeared with a peak around 490 nm once the material was irradiated. It is noteworthy that new luminescent centers were generated by the irradiation. These results clearly demonstrate that Eu:$KCaPO_4$ exhibits RPL upon X-ray irradiation.

The origin of the RPL was next investigated. Figure 3(a) shows the PL excitation spectra of all specimens around the peak emission at 610 nm. The excitation spectra corresponding to the emission at 610 nm consists of a broad excitation band in the range of 200–300 nm and discrete sharp peaks in the range of 300–500 nm. The broad excitation band in the range of 200–300 nm is attributed to the charge transfer (CT) transition from the filled 2*p* shell of O^{2-} to the partially filled 4*f* shell of Eu^{3+}.[21] In the range of 350 to 500 nm, all specimens exhibited intra-configurational 4*f*–4*f* transitions of Eu^{3+}: 299 nm ($^7F_0$–$^5H_6$), 319 nm ($^7F_0$–$^5H_3$), 362 nm ($^7F_0$–$^5D_4$), 369–378 nm ($^7F_0$–^5G_J), 381 nm ($^7F_0$–$^5L_6$), 415 nm ($^7F_1$–$^5D_3$), and 465 nm ($^7F_0$–$^5D_2$).[21] The excitation spectral intensity attributed to the 4*f*–4*f* transitions of each Eu^{3+} monotonically increased with increasing Eu concentration in the specimens. Figure 3(b) shows the PL excitation spectra of all specimens around the peak at 490 nm after irradiation with 10 Gy of X-rays. The

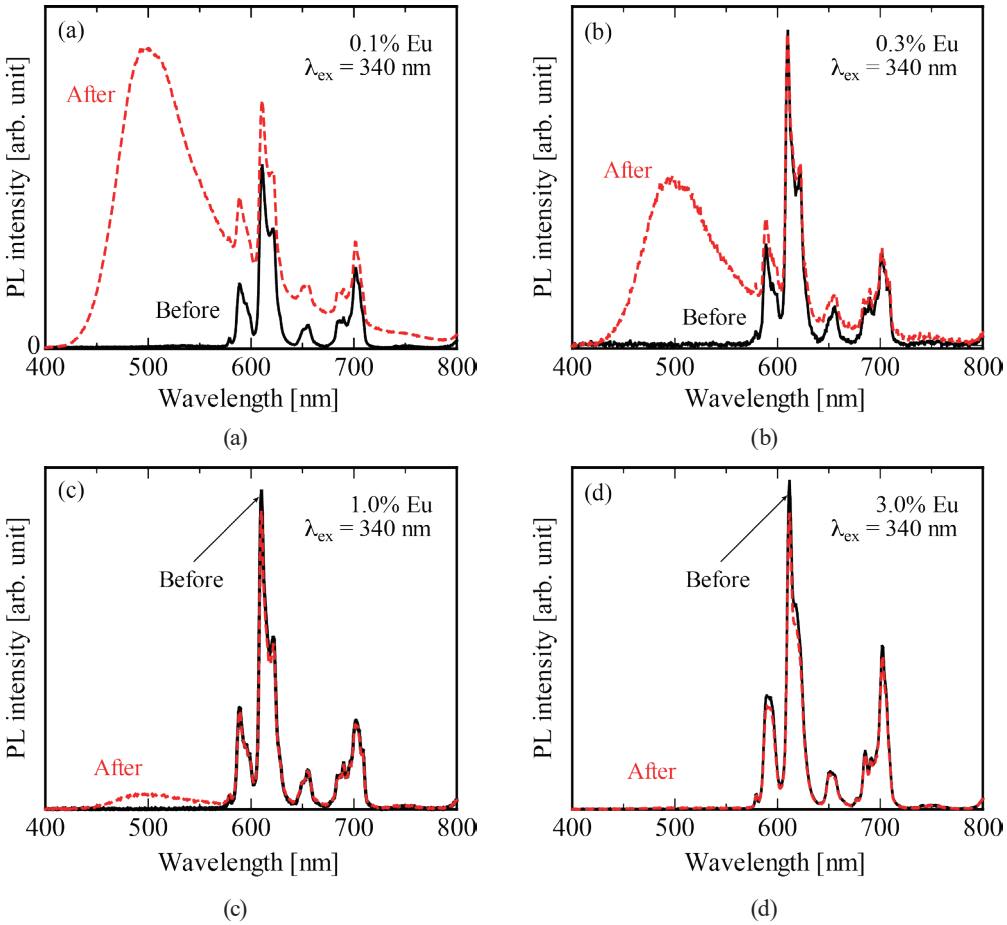

Fig. 2. (Color online) PL spectra of the (a) 0.1, (b) 0.3, (c) 1.0, and (d) 3.0% Eu-doped specimens measured before and after X-ray irradiation (10 Gy). The excitation wavelength was 340 ± 20 nm.

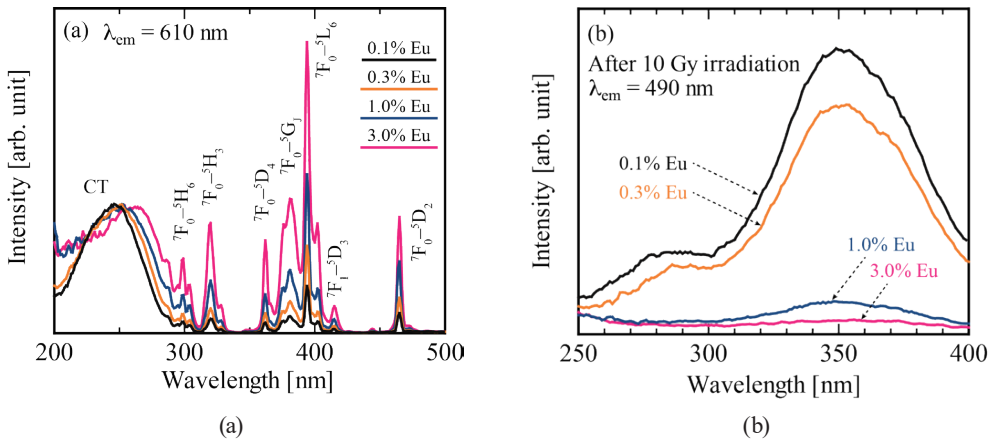

Fig. 3. (Color online) Excitation spectra of all specimens obtained at (a) 610 nm before X-ray irradiation and (b) 490 nm after X-ray irradiation.

obtained excitation spectra showed concentration dependence; the most pronounced excitation band was observed in the 0.1% Eu-doped specimen with the lowest Eu concentration, and the spectral intensity decreased with increasing Eu concentration.

Figure 4 shows PL decay features of the (a) line emissions peaking at 610 nm and (b) broad emission peaking at 490 nm, and the obtained PL lifetime constants are summarized in Table 1. The excitation wavelengths were 265 and 340 nm, respectively. Both the decay curves can be approximated well by the single exponential function

$$I(t) = A\exp\left(-\frac{t}{\tau}\right), \tag{1}$$

where I and A are the luminescence intensities at times t and 0, respectively, and τ is the luminescence lifetime. The PL lifetime was obtained as 2.34–2.72 ms for the 610 nm emission and 750–625 ns for the 490 nm emission. The PL lifetime of the line emission peaking at 610 nm is reasonable for the $4f$–$4f$ transition of the Eu^{3+} ion, which is known to be several milliseconds.[21,22] Furthermore, the PL lifetime increases with increasing Eu concentration in the specimens. On the other hand, the PL lifetime of the broad emissions peaking at 490 nm was a few microseconds in all specimens.[16,20] The results are in good agreement with the values attributed to the $4f^6 5d^1$–$4f^7$ transition of Eu^{2+}, suggesting that the broad emission induced by X-ray irradiation is due to the Eu^{2+}. In contrast to the PL lifetime of the 610 nm emission, the PL lifetime of the 490 nm emission decreases with increasing Eu concentration in the specimens.

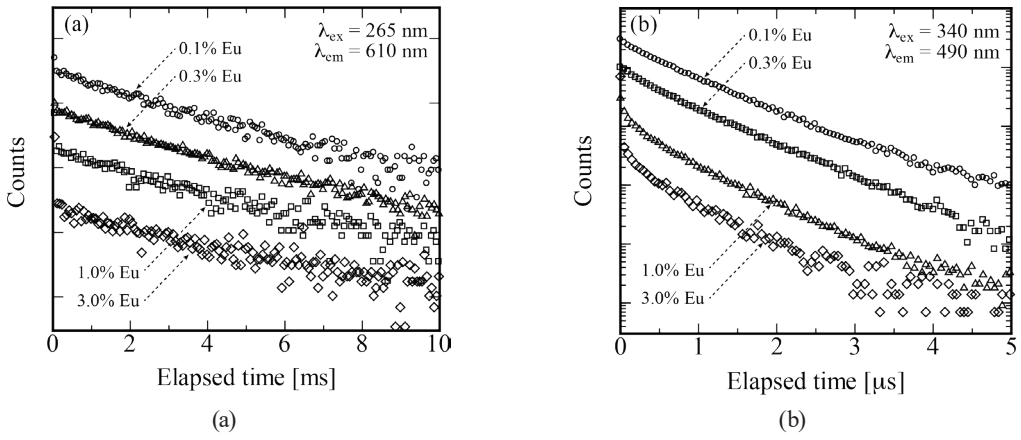

Fig. 4. PL decay curves measured by monitoring the emissions at (a) 610 nm before X-ray irradiation and (b) 490 nm after X-ray irradiation. The excitation wavelength for each emission was (a) 265 nm and (b) 340 nm.

Table 1
PL lifetimes of the Eu:$KCaPO_4$ specimens. The excitation wavelengths corresponding to 610 and 490 nm emissions were 265 and 340 nm, respectively. The excitation light was cut off from the light source by an optical filter.

Specimen	PL lifetime (ms)/610 nm emission	PL lifetime (ns)/490 nm emission
0.1% Eu	2.34	750
0.3% Eu	2.40	712
1.0% Eu	2.45	627
3.0% Eu	2.72	625

The relationship between the X-ray dose and the corresponding PL intensity measured for Eu^{3+} and Eu^{2+} is shown for each Eu-doped specimen in Fig. 5. These results illustrate that with increasing X-ray dose, the PL intensity of Eu^{3+} decreased and the intensity of Eu^{2+} increased in all the specimens. Focusing on the dynamic range for each specimen, we can see that as the Eu concentration in the specimens increased, the dose threshold at which Eu^{2+} is generated increased. The RPL in this specimen is due to the valence change from Eu^{3+} to Eu^{2+}, and it is assumed that the Eu^{3+} ions in the $KCaPO_4$ capture electrons generated by X-rays to form Eu^{2+}. In order for Eu^{2+} not to recapture holes, there must be stable hole-trapping centers in the host material whose trapping probability must be high. In view of this, it is considered that the hole-trapping probability was high and there were many trapping centers in the 0.1% Eu-doped specimen, whose number decreased with increasing Eu concentration. The results of TSL glow curve measurements performed to verify these hypotheses are next given.

The TSL glow curve represents the luminescence intensity as a function of temperature while heating at a constant rate. Prior to the measurement, the specimens were irradiated with X-rays. The obtained glow curves are shown in Fig. 6. The 0.1% Eu-doped specimen showed pronounced TSL in the range of 80–300 °C, but the intensity markedly decreased with increasing Eu concentration, with almost no TSL observed for the 1.0 and 3.0% Eu-doped specimens. In the

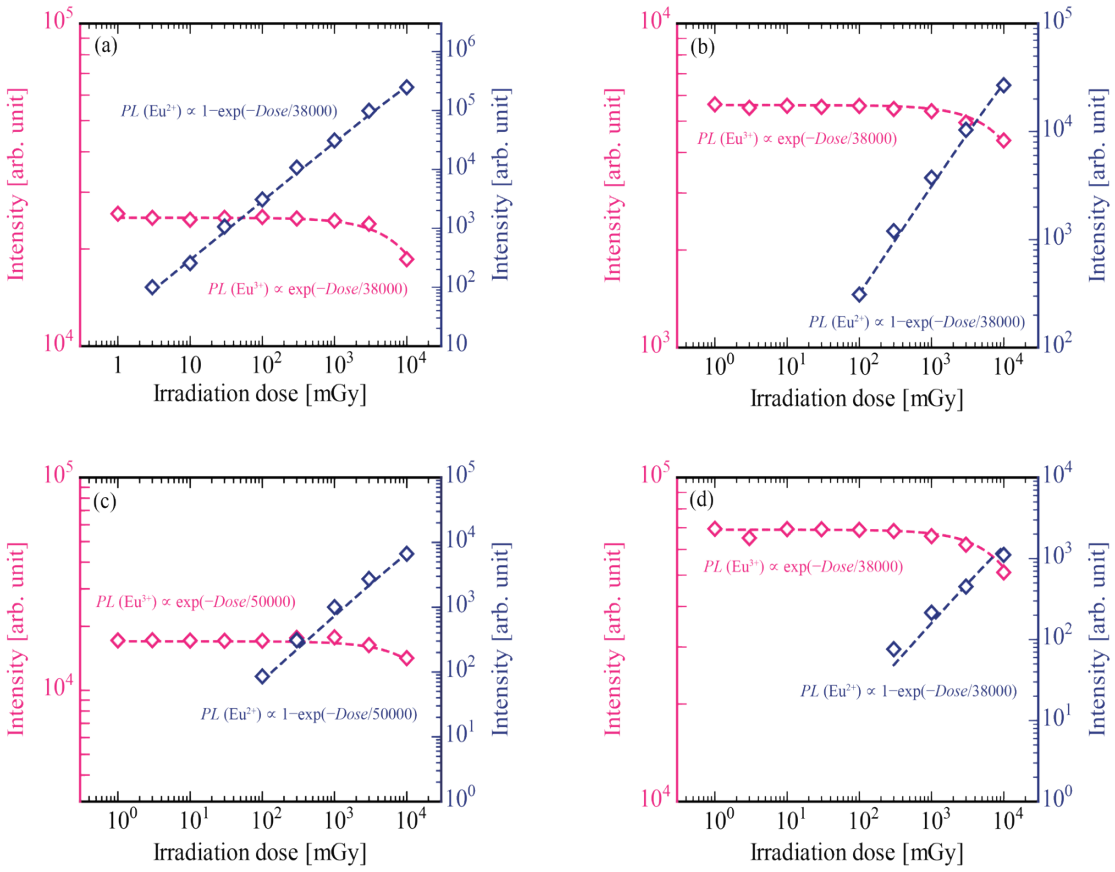

Fig. 5. (Color online) PL intensities of Eu^{3+} and Eu^{2+} in all specimens as a function of irradiated X-ray dose.

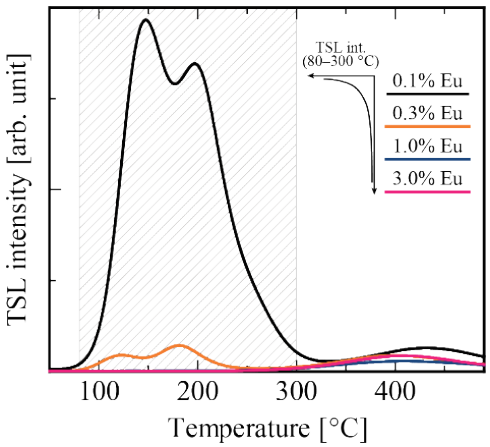

Fig. 6. (Color online) TSL glow curves of all the specimens after X-ray irradiation.

range of 300–490 °C, no significant differences in the glow curve shape were observed among the specimens with different Eu concentrations. As one of the reasons for the high luminescence intensity in the TSL glow curve, it is considered that the total number of trapped electrons or holes in the specimens was large. In this case, the stability of Eu^{2+} depends on the probability that Eu^{3+} captures an electron and then captures a hole. Therefore, the higher the number of holes captured, the greater the stability of Eu^{2+}. In other words, RPL is most likely to occur in the 0.1% Eu-doped specimen, which contains the most trapping centers, and least likely to occur in the 3.0% Eu-doped specimen.

4. Conclusions

$K(Eu_xCa_{1-x})PO_4$ (x = 0.001, 0.003, 0.01, and 0.03) ceramics were synthesized by the conventional solid-state reaction. Peaks of $KCaPO_4$ and β-$KCaPO_4$ were found to coexist in the XRD patterns of all the Eu-doped specimens. The PL spectrum of each specimen showed only characteristic emissions attributed to the $4f$–$4f$ transition of Eu^{3+}, whereas additional broad emission attributed to the $5d$–$4f$ transition of Eu^{2+} appeared after X-ray irradiation. RPL emission was pronounced in the 0.1% Eu-doped specimen and decreased with increasing Eu concentration. From the analysis of the TSL glow curves, it was found that the number of RPL-producing centers was correlated with the number of hole-trapping centers in the specimen. Elucidation of the mechanism in more detail will require analysis of, for example, the coordination structure.

Acknowledgments

This work was supported by Grants-in-Aid for Scientific Research A (17H01375), B (18H03468 and 19H03533), Early-Career Scientists (20K20104), and JSPS Fellows (20J23225). The Cooperative Research Project of Research Center for Biomedical Engineering is also acknowledged.

References

1 T. Yanagida, H. Masai, M. Koshimizu, and N. Kawaguchi: Sens. Mater. **31** (2019) 1225.
2 M. Koshimizu, T. Yanagida, R. Kamishima, Y. Fujimoto, and K. Asai: Sens. Mater. **31** (2019) 1233.
3 Y. Takebuchi, H. Fukushima, T. Kato, D. Nakauchi, N. Kawaguchi, and T. Yanagida: Sens. Mater. **32** (2020) 1405.
4 D. Shiratori, D. Nakauchi, T. Kato, N. Kawaguchi, and T. Yanagida: Sens. Mater. **32** (2020) 1365.
5 T. Kato, D. Nakauchi, N. Kawaguchi, and T. Yanagida: Sens. Mater. **32** (2020) 1411.
6 A. J. J. Bos and J. B. Dielhof: Radiat. Prot. Dosimetry **37** (1991) 231.
7 V. E. Kafadar and K. F. Majeed: Thermochim. Acta **590** (2014) 266.
8 S. W. S. McKeever: Radiat. Meas. **46** (2011) 1336.
9 C. B. Palan, N. S. Bajaj, and S. K. Omanwar: Int. Conf. Condens. Matter Appl. Phys. (2016) 020474.
10 D. Y. C. Huang and S. M. Hsu: Adv. Cancer Ther. (InTech, 2011).
11 G. Okada, Y. Fujimoto, H. Tanaka, S. Kasap, and T. Yanagida: J. Rare Earths **34** (2016) 769.
12 G. Okada, K. Shinozaki, T. Komatsu, S. Kasap, and T. Yanagida: Radiat. Meas. **106** (2017) 73.
13 D. Shiratori, Y. Isokawa, H. Samizo, N. Kawaguchi, and T. Yanagida: J. Ceram. Soc. Jpn. **127** (2019) 455.
14 C. B. Palan, K. A. Koparkar, N. S. Bajaj, A. Soni, and S. K. Omanwar: Res. Chem. Intermed. **42** (2016) 7637.
15 C. Malik, A. Pandey, and B. Singh: Integr. Ferroelectr. **204** (2020) 73.
16 S. Zhang, Y. Huang, and H. J. Seo: J. Electrochem. Soc. **157** (2010) J261.
17 T. Yanagida, Y. Fujimoto, N. Kawaguchi, and S. Yanagida: J. Ceram. Soc. Jpn. **121** (2013) 988.
18 D. K. Yim, I.-S. Cho, C. W. Lee, J. H. Noh, H. S. Roh, and K. S. Hong: Opt. Mater. **33** (2011) 1036.
19 M. A. Bredig: J. Phys. Chem. **46** (1942) 747.
20 L. Guan, C. Liu, X. Li, G. Jia, Q. Guo, Z. Yang, and G. Fu: Mater. Res. Bull. **46** (2011) 1496.
21 R. Yu, H. Li, H. Ma, C. Wang, and H. Wang: Solid State Sci. **29** (2014) 34.
22 S. Zhang, Y. Nakai, T. Tsuboi, Y. Huang, and H. J. Seo: Chem. Mater. **23** (2011) 1216.